



## PREDICTION OF CANOPY COVER FOR AGRICULTURAL LAND CLASSIFICATION IN LAND PARCEL IDENTIFICATION SYSTEM (LPIS) DATA USING PLANET-SCOPE MULTISPECTRAL IMAGES: A CASE STUDY OF GELENDOST DISTRICT

Sinan DEMİR<sup>1\*</sup>

<sup>1</sup>Isparta University of Applied Sciences, Faculty of Agriculture, Department of Soil Science and Plant Nutrition, 32200, Isparta, Türkiye

**Abstract:** Determining canopy cover (CC) temporal variation is critical for sustainable management of natural resources and environmental protection efforts. Data analysis and interpretation methods for remote sensing are important for understanding these changes and adapting to natural systems. In this study used the Parcel Identification System (LPIS) database physical blocks as field ground data. In the study area, agricultural areas were determined from LPIS data, including classes A0, A1, A3, A4, S1, T0, and T1, and a total of 8424 physical blocks and an area of 14651.9 hectares were evaluated. CC estimates were made using 3-m spatial resolution Planet Scope multispectral satellite images of July and August 2023, and it was determined that there were significant differences in parcel-based distinctions, especially in parcels A0, A1, T0, and T1 ( $P<0.05$ ). According to the study results, it was determined that using the estimated CC data, the A0 (69.27%) and T0 (30.43%) land cover types could be successfully used to determine the changes in the phenological period caused by environmental impact assessment such as climate change. At the same time, this study contributes to the rapid monitoring of agricultural production areas caused by climate change by using physical blocks of agricultural land classes within the LPIS data, the rapid determination of agricultural land management, and support payments with remote sensing data. In this regard, the use of modern technologies and data analysis methods will contribute to increasing agricultural sustainability.

**Keywords:** Land use/land cover, Canopy cover, NDVI, LPIS, Climate change, Remote sensing

\*Corresponding author: Isparta University of Applied Sciences, Faculty of Agriculture, Department of Soil Science and Plant Nutrition, 32200, Isparta, Türkiye

E-mail: sinandemir@isparta.edu.tr (S. DEMİR)

Sinan DEMİR  <https://orcid.org/0000-0002-1119-1186>

Received: May 27, 2024

Accepted: July 04, 2024

Published: July 15, 2024

Cite as: Demir S. 2024. Prediction of canopy cover for agricultural land classification in land parcel identification system (LPIS) data using planet-scope multispectral images: A case study of Gelendost district. BSJ Agri, 7(4): 407-417.

### 1. Introduction

Population increase and climate change have a significant impact on the dynamics of natural ecosystems and agricultural areas (Demir, 2024). Understanding and monitoring these changes are crucial for preserving natural ecosystems and ensuring agricultural sustainability. Remote sensing techniques offer effective methods for monitoring these changes (Demir, 2023).

Multispectral remote sensing programs, such as Landsat, Sentinel, Spot, IKONOS, WorldView, GeoEye, KOMPSAT, SkySat, MODIS, Gaofen, Pleiades, and PlanetScope, provide crucial spectral data across various regions of the electromagnetic spectrum (Vos et al., 2019). These data offer insights into plant properties such as leaf pigment concentration, water content, and internal structure, contributing to the effectiveness of remote sensing applications in agricultural and biodiversity research (Selim and Sönmez, 2015; Damm et al., 2018; Hatfield et al., 2019; Berger et al., 2022; Selim et al., 2022; Esetili et al., 2022; Le et al., 2023; Demir et al., 2024; Aljanabi et al., 2024; Demir and Başyayğıt, 2024).

Vegetation dynamics play a pivotal role in agricultural

productivity, providing insights into plant health and growth. Canopy cover (CC), which represents the proportion of ground covered by photosynthetically active vegetation, is a key indicator of plant growth and health (Tucker, 1979; Pei et al., 2018). This metric is widely utilized in various applications, including crop canopy growth measurement, radiation interception, and evapotranspiration partitioning in hydrological and agricultural modeling (Trout et al., 2008; Talsma et al., 2018; Ghiat et al., 2021; Tenreiro et al., 2021; Qin et al., 2023; Oliveira et al., 2024).

The Normalized Difference Vegetation Index (NDVI) is a commonly used tool for defining CC and is employed in both proximal and remote sensing methods (Tenreiro et al., 2021; Carella et al., 2024; Theime et al., 2024). In addition, several other vegetation indices have been developed alongside the NDVI to characterize vegetative diversity. Many indices have been created to characterize vegetative diversity in addition to the NDVI (Rouse et al., 1974; Huete, 1988; Clevers, 1989; Baret and Guyot, 1991; Pinty and Verstraete, 1992; Kaufman and Tanre, 1992; Rondeaux et al., 1996; Basso et al., 2004; Gitelson, 2013; Hassan et al., 2018; Kumar et al., 2018). Despite



theoretical promises of improvement over NDVI in addressing soil background and atmospheric influences, NDVI remains widely used due to its accessibility and user-friendliness across satellite and remote sensing platforms (Rondeaux et al., 1996; Gitelson, 2013; Hassan et al., 2018; Gong et al., 2023; Kumar et al., 2024; Demir et al., 2024). Remote sensing-based CC estimation is becoming increasingly useful for calibrating models in spatial analysis of cropping systems. Effective CC estimation models can be created using the multispectral image's NDVI and other vegetation indices. This approach is less expensive and requires less time than standard in situ measurements. Trout et al. (2008) used a handheld multispectral digital camera to measure the canopy cover of 11 different horticultural crops in 30 fields on the west side of California's San Joaquin Valley. They compared the results with NDVI values computed from Landsat 5 satellite images. The study found a strong correlation ( $R^2=0.95$ ,  $P<0.01$ ) between NDVI and canopy cover, with an average absolute error of 0.047 up to complete coverage. Tsakmakis et al. (2021) established an effective model for assessing canopy cover (CC) in maize fields. They examined the link between the NDVI values obtained from the Sentinel satellite images and the on-site CC, obtaining an  $R^2$  greater than 0.98. Thieme et al. (2024) studied the comparability between ground-based and spaceborne sensors for assessing the biophysical characteristics of winter cover crops. Their research focused on measuring biomass and fractional vegetative groundcover using SPOT 5, Landsat 7, WorldView-2 satellite imagery, and handheld multispectral proximate sensors. They found that surface reflectance imagery demonstrated greater associations with proximal sensors than with top-of-atmosphere data. Surface reflectance NDVI showed high agreement with proximate sensor-derived fractional green cover and biomass, with modified  $R^2$  values of 0.96 and 0.95. Studies have repeatedly revealed a strong association between CC and NDVI, although this relationship may differ among crop species. Standardized correlations are consequently required to reduce uncertainty when

forecasting CC using the NDVI. Despite these limitations, NDVI remains a valuable tool for estimating vegetation characteristics.

In summary, NDVI-derived vegetation indices using multispectral remote sensing data provide a viable method for quantifying canopy cover and understanding vegetation dynamics. These indexes help improve the accuracy of agricultural and environmental responses to climate change by supporting the development of canopy cover prediction models.

The aim of this study was to determine the possibility of merging Parcel Identification System (LPIS) data with high-resolution satellite images to evaluate canopy cover in LPIS-based subsidy programs. In addition, we intend to investigate these inconsistencies at the parcel level by using canopy cover data to address variations in the phenological stages in response to weather differences. The results of this study can have a substantial impact on agricultural policies and encourage the adoption of sustainable farming practices.

## **2. Materials and Methods**

### **2.1. Field Description**

The study area is located within the borders of the Gelendost district in the province of Isparta in Türkiye's Lakes Region. It extends between coordinates 310725–340359 east and 4202796–4232165 north (Zone 36, UTM-m) (Figure 1). The Gelendost district, which covers the study area, has a surface area of 610.95 km<sup>2</sup>, according to the General Directorate of Maps. The district is located 81 kilometers from Isparta's center at an elevation of 913–2213 m. Positioned on the eastern side of the Eğirdir lake, the district experiences a transition between Mediterranean and Central Anatolian climates. Mediterranean climate effects are prominent in low-lying areas because of the lake effect, transitioning to a cooler and rainy climate with increased altitude toward the mountains. The study area, located near the Eğirdir lake, has experienced an average total precipitation of 433.2 mm and an average temperature of 14.5 °C for many years (1990–2020) (MGM, 2024).

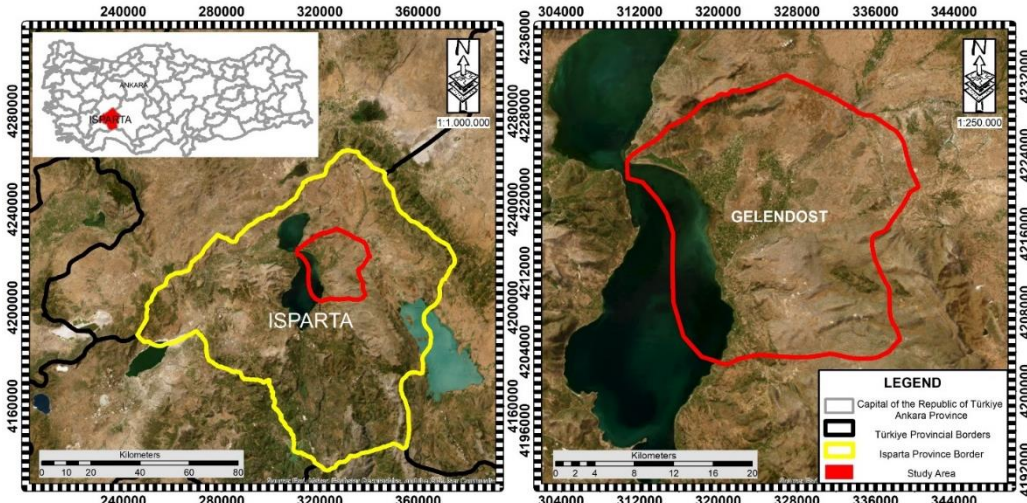


**Figure 1.** Study area location map.

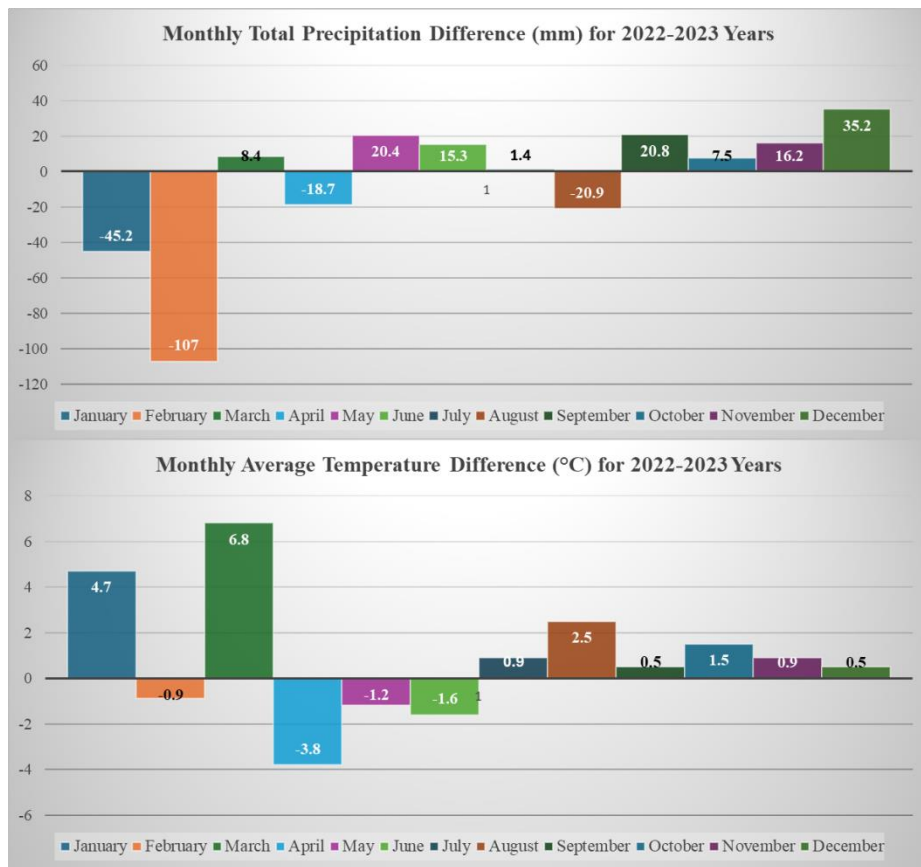


**Figure 2.** Changes in precipitation and temperature regimes for the years 2022-2023 in the study area.

The distribution of agricultural land use in the study area in 2023 by product group was determined. Within the farmland of fruits, beverages, and spice plants, apples are produced at 91.7%. In the farmland of vegetables, garlic accounts for 41.9%, with 12.6% being tomatoes, 11.2% being melons, 8.9% being cucumbers, and 5.6% being bean production. In the farmland of grains and other plant products, 42% consists of durum wheat, 35% barley, and 10.5% safflower production (TurkStat, 2024).

## 2.2. Climate Data

Climate data plays a crucial role in agricultural production, affecting various aspects of crop cultivation. It influences phenological dates, delaying the maturation of annual crops and affecting the flowering period in fruit orchards, thereby influencing fruit set and quality (Çakır et al., 2021; Yalçın et al., 2021; Yılmaz et al., 2021; Kazemi et al., 2023; Ličina et al., 2024). The impact of climate parameters on agriculture directly influences the plant growth cycle, harvest timing, and productivity. The monthly average temperature and precipitation data for the study area in 2022 and 2023 were obtained from station number 18114 of the General Directorate of Meteorology (MGM, 2024). Monthly variations are shown in Figure 2.

In 2022, there was 441.4 mm of precipitation overall; in 2023, there was 374.8 mm. As a result, 2023's total precipitation was 66.6 mm less than 2022's. Thus, the increase in temperature data is influenced by the decrease in precipitation. In 2022 and 2023, the annual

average temperature was 13.2°C and 14.1 °C, respectively. As a result, the average temperature in 2023 rose by 0.9 °C over 2022.

## 2.3. Land Parcel Identification System Database

One of the main components of the European Union's IACS (Integrated Administration and Control System) is the Land Parcel Identification System (LPIS), a system that precisely defines each and every agricultural land parcel in member states. Up until 2003, member countries mandated its use. Under the scope of EU membership negotiations, Türkiye began implementing LPIS in 2003. In 2016, LPIS data for the entire nation were established using physical block reference systems (Anonymus, 2024). There are five-year updates to the LPIS data (Simşek and Durduran, 2022). The administration of agricultural land, assistance payments, and the execution of environmental protection measures all heavily depend on this update. The parcel data used in this analysis were obtained from the LPIS database. The LPIS database's agricultural land cover categories allowed us to choose classes that corresponded to arable areas for our study. The classes of land use status within the study area of the LPIS data are as follows: arable land (A0), arable land with sparse (scattered) trees (A1), mixed agricultural regions (A3), greenhouses (A4), continuous bush product: vineyards (S1), continuous wood products (T0), and permanent wood product: olive trees. Table 1 shows the distribution of classes in the study area within Türkiye's borders (Anonymus, 2024).

**Table 1.** Spatial distribution of agricultural parcel classes according to LPIS data in Türkiye

Code	Name	Physical Block Count	Surface Area (Km <sup>2</sup> )
A0	Arable land	3598752	192953.41
A1	Arable land with scattered trees	24271	433.27
A3	Mixed agricultural areas	38271	31.22
A4	Greenhouses	76137	438.03
S1	Permanent shrub crops: Vineyards	157931	2695.61
T0	Permanent tree crop	943607	14545.74
T1	Permanent tree crop: Olive trees	146647	577.74

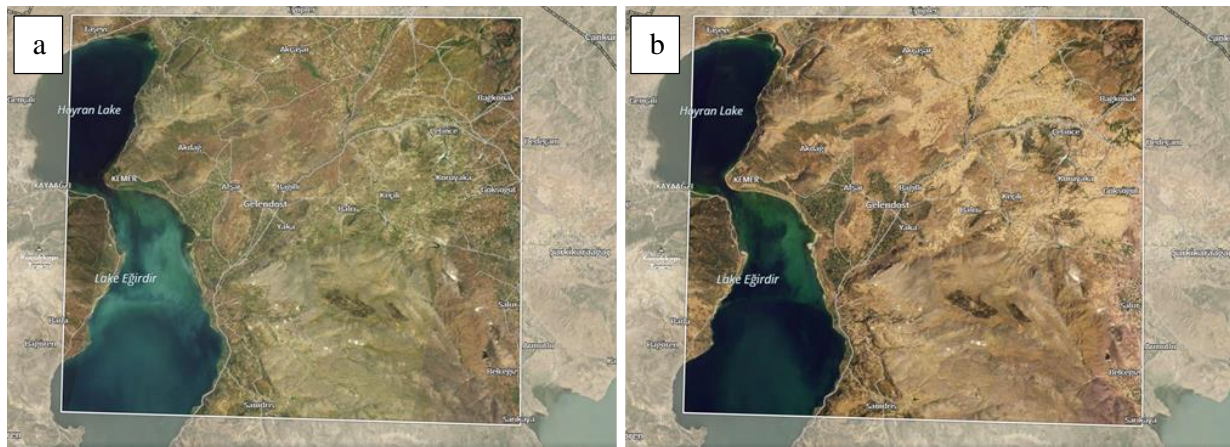


**Figure 3.** Orthorectified image (a) July 4, 2023 (b) August 24, 2023.

#### 2.4. Data Collection and Preprocessing

With 120 satellites in orbit, the Planet-Scope constellation is the largest commercial satellite fleet in history, capturing images of the entire Earth's surface every day (Ghuffar, 2018). With a resolution of 3–5 m, its sensors can capture images in four different multispectral bands: red, green, blue, and near-infrared. This makes it ideal for monitoring and assessing changes in the amount of plant and forest cover. Data from the commercial satellite Planet-Scope are available for purchase from Planet Inc. or can be downloaded for free for academic use (Team, 2017; Planet, 2024).

In our study, Planet-Scope imagery covering the study area, which extends between the coordinates 305526–351372 east and 4201685–4238913 (Zone 36, UTM-m), acquired on July 4 and August 24, 2023, was used. Figure 3 shows the product Level 3B images (Planet, 2024), which encompass the study area and were acquired on two different dates.

Satellite imagery is retrieved under different levels, with each level requiring necessary corrections before further processing. Our retrieved satellite imagery is 'Surface Reflectance' in the case of Planet-Scope Dove, already corrected for radiometric and atmospheric corrections (Planet, 2024). All the data have the same pixel size of 3 m.

Vegetation index, such as NDVI, is a measure of the health of a plant based on how the plant reflects light at certain frequencies (Rouse et al., 1974). The NDVI was calculated for the Planet-Scope imagery using Erdas Imagine software (Erdas, 2024), according to the equation given

in Equation 1. The canopy cover was then calculated according to the model proposed by Trout and Johnson (2007), as given in Equation 2.

$$NDVI = \frac{(NIR - RED)}{(NIR + RED)} \quad (1)$$

$$Canopy\ Cover\ (\%) = (1.22 * NDVI - 0.21) * 100 \quad (2)$$

After calculating the canopy cover, the determined LPIS physical block parcels within the study area were analyzed using the Zonal Statistics tool in ArcGIS software (Demir et al., 2024). A dataset for 8388 parcels was created, including pixels' data. Canopy cover pixel values were determined for the LPIS dataset within land cover types such as arable land (A0), arable land with sparse (scattered) trees (A1), mixed agricultural regions (A3), greenhouses (A4), continuous bush product: vineyards (S1), continuous wood products (T0), and permanent wood product: olive trees (T1).

#### 2.5. Statistical Analyses

The study was conducted based on the different types of land uses for LPIS parcels, and a frequency distribution analysis was carried out. The study used the Global Moran's I statistic to examine spatial autocorrelation and calculated a Moran's Index of 0.833 (Figure 4). This index, along with a z-score of 78.285 and a p-value of 0.000, signifies a clustered pattern with a probability of less than 1% of occurring randomly. These results point to a nonrandom spatial distribution within the dataset, indicating that underlying variables may be influencing observable clustering patterns. In addition, a one-sample Kolmogorov-Smirnov test of normality confirmed the

null hypothesis of normal distributions. In this study, box-plot statistics were computed on the basis of land cover types in the LPIS dataset using satellite imagery collected in two periods. The estimated canopy cover values for each period were determined at the parcel scale using the Zonal Statistics tool. Descriptive statistical results were then derived. Within the study area, mean canopy cover values for different periods were calculated on the basis of LPIS data corresponding to agricultural land cover types A0, A1, A3, A4, S1, T0, and T1. Levene's test of homogeneity of variance for zone types revealed significant differences ( $P < 0.05$ ); hence, the conservative Tukey test, with significance measured at  $\alpha = 0.05$ , was employed for post hoc comparisons. This analysis involved 8388 different parcel scale observations across seven parcel types. ArcGIS software (ArcGIS, 2024) was used for geographic data processing, Erdas Imagine software (Erdas, 2024) for processing 3-m spatial resolution Planet-scope imagery, and statistical analyses of the resulting database were performed using the Minitab software package (Minitab, 2024).

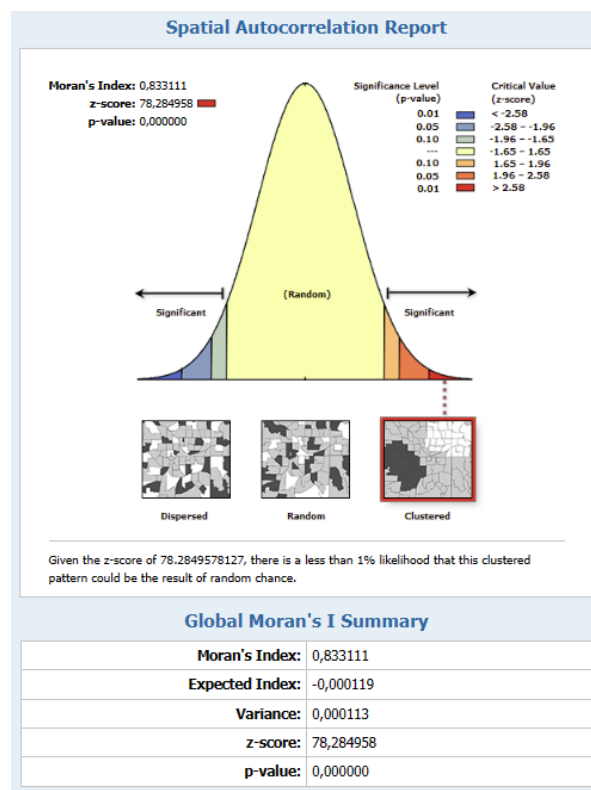


**Figure 4.** Moran I index of physical blocks in the study area.

### 3. Results

#### 3.1. Study Area LPIS Database

The analysis of the LPIS data indicated land use patterns that are crucial in enhancing agricultural output. Proper classification and usage of agricultural lands, particularly in high-productivity zones, aids in the optimization of production amounts. Furthermore, by tracking land use changes, these spatial data help promote sustainable agriculture practices. Enable land use data served as field

ground data for the study area LPIS data. Table 2 shows the number of parcels and their spatial distribution in the research region for land cover classes A0, A1, A3, A4, S1, T0, and T1. Parcels labeled A0 represent the agricultural areas with the largest area in the research region. It has the largest area of 10149.07 ha, accounting for 69.27% of the total research area. The number of physical blocks indicates that such lands are broad and dispersed over large areas. The relatively high standard deviation indicates that such plots differ in size. General agricultural lands are broad areas where herbaceous crops, including cereals, legumes, and oilseeds, are farmed (Table 2). Parcels coded A1 are among the smallest farmlands in the study area. They account for only 0.08% of the study area, totaling 12.30 hectares. The lower number of physical blocks indicates that this sort of land is less common. The low standard deviation (0.601) indicates that the plot sizes are reasonably comparable (Table 2). A3 coded parcels are one of the farmlands with the smallest surface area, totaling 4.30 hectares and accounting for only 0.03% of the total area. The low number of physical blocks indicates that such regions are uncommon. The standard deviation is relatively low, indicating that such plots are very similar in size (Table 2). A4 coded parcels cover a small area of 4.23 hectares or 0.03% of the total area. The small number of physical blocks indicates that these farmlands are scarce. The low standard deviation indicates that the plot sizes are quite similar. Greenhouses mitigate the detrimental consequences of climate change by creating controlled environments (Table 2). Parcels coded S1 covers 1.06% of the research area, totaling 20.36 ha. These farmlands, with a physical block number of 20, are clustered in specific locations (Figure 3). The standard deviation number (1.064) indicates that the sizes are quite close together (Table 2). Parcels coded T0 covers a considerable area, totaling 4458.87 ha, or 30.43% of the total area. The large number of physical blocks indicates that such areas are relatively frequent. The relatively high standard deviation indicates that such plots vary in size (Table 2). Parcels code T1 covers a small area of 2.73 ha or 0.02% of the total area. The small number of physical blocks indicates that these territories are scarce. The low standard deviation indicates that the plot sizes are quite similar. In total, the study area includes 8388 physical blocks and 14,651.9 hectares of agricultural land. The largest area consists of agricultural lands with code A0, and the smallest area consists of special-use agricultural fields with codes A3 and A4. This distribution demonstrates that agricultural activities are primarily focused on large, general agricultural businesses. In addition, different land use forms appear to differ greatly in size and scope. Figure 5 shows the spatial distribution of the LCT code and physical block data from the LPIS dataset in the study area.

**Table 2.** Study area and agricultural parcel status according to the LPIS database

LCT Code	Physical Block Count	Area (Hectare)	Standard Deviation	Area (%)
A0	5425	10149.07	69.27	2.343
A1	19	12.30	0.08	0.601
A3	26	4.30	0.03	0.092
A4	13	4.23	0.03	0.305
S1	20	20.36	0.14	1.064
T0	2878	4458.87	30.43	2.246
T1	7	2.73	0.02	0.249
Total	8388	14651.9	-	100

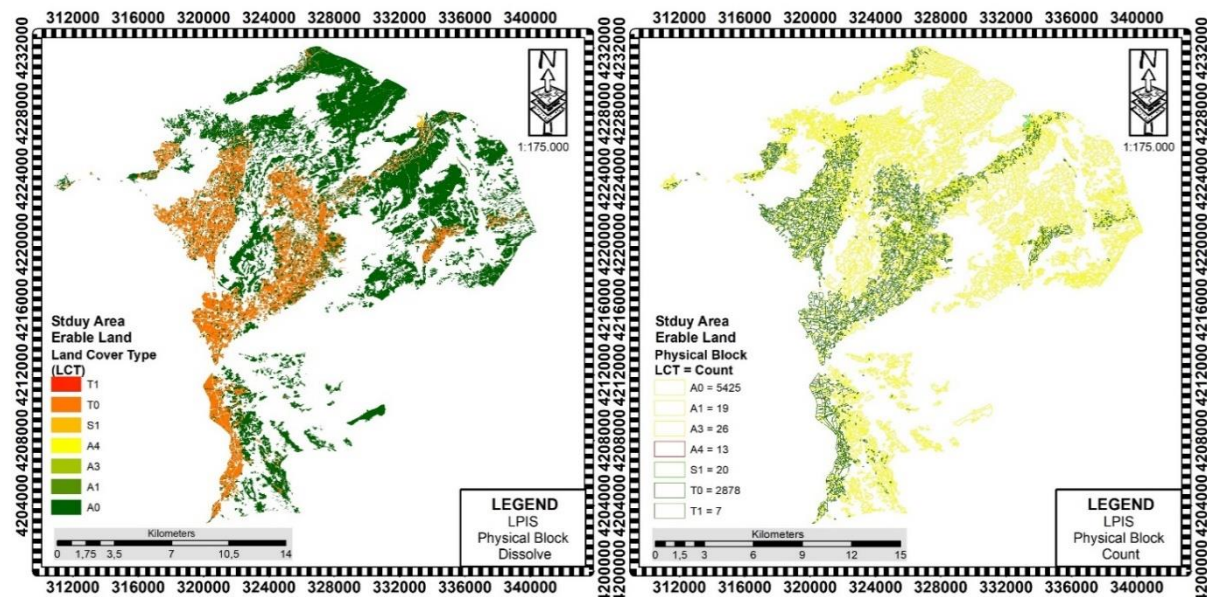


**Figure 5.** Study area agriculture parcel physical blocks spatial distribution.

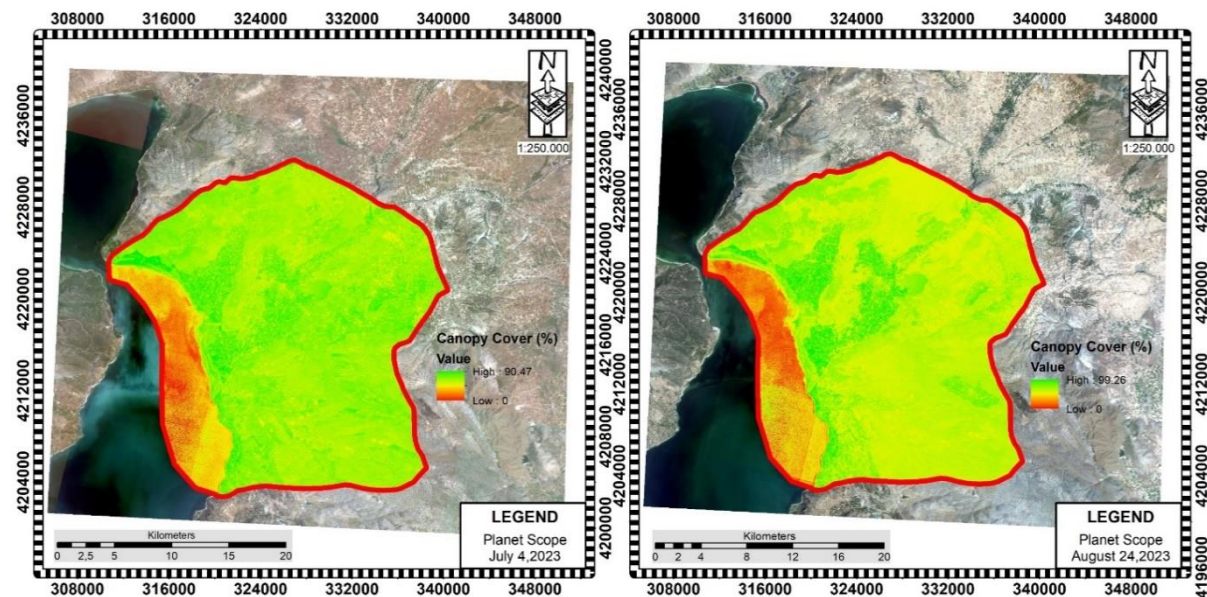


**Figure 6.** Study area canopy cover prediction at different temporal resolutions.

### 3.2. Canopy cover prediction

In this study, the CC of agricultural areas in the study area was estimated using high-resolution PlanetScope satellite images with varying temporal resolutions. Changes in the vegetation period due to changes in the

study area's climatic circumstances resulted in considerable changes in the CC data (Figure 6). These changes were evaluated using the LCT (Land Cover Types) physical block types from the LPIS data, and the descriptive statistics results are shown in Table 3. Table

3 shows descriptive statistics for canopy cover percentages based on different LCT types, including minimum, mean, maximum, standard deviation, coefficient of variation, skewness, and kurtosis values. These statistics provide important information for understanding and evaluating the CC distribution of different LCT categories in the study area. The estimated CC values in the first and second periods show significant changes in different LCT codes. While in the first period, code A0 had the highest average CC value (33.53), this value decreased significantly (21.16) in the second period. In addition, the skewness and kurtosis values in the A0 code shifted, indicating that the distribution's asymmetry and kurtosis characteristics had changed. It is worth noting that in the A1 code, the average values are low in both periods, as are the skewness values; this indicates that the distribution has a long tail to the right, resulting in more extreme results. While the average values in the A3 and S1 codes are similar in both eras, the average and coefficient of variation in the A4 category are much lower and higher. In the T0 and T1 codes, a larger distribution and increased standard deviation values were observed in the second period, indicating that environmental variables and agricultural methods have considerable effects on canopy cover across time. As a result, the A0 and T0 codes show a more homogenous distribution, whereas the A1 and A4 codes show higher variability and skew. In the T0 code, the canopy cover percentage had a high average value and a homogeneous distribution with low skewness and kurtosis. This demonstrates that the T0 code contains dense and regular vegetation in the research area.

Figure 6 shows the spatial distribution of July and

August's estimated canopy cover levels. These spatial distribution maps depict the effects of changes in vegetation phase and meteorological conditions on canopy coverage. Data collected in July and August are crucial for a better understanding of temporal changes in CC estimates and the impact of agricultural operations in the study area. While CC values increase in well-structured covered orchards within the study area, Figure 6 shows the spatial distribution of the decline in canopy value in dry-farmed areas where annual plants are planted.

This study investigated the impact of canopy cover values estimated across different time periods on land cover in agricultural areas. The Kolmogorov-Smirnov normality test results indicated that the average results of the physical blocks for the estimated canopy cover values followed a normal distribution. Average canopy cover values for each LCT (Land Cover Type) type were investigated using post hoc tests such as analysis of variance and the Tukey test at a 95% confidence interval. Analyses revealed that canopy cover values varied significantly among vegetation periods (Table 4). These discrepancies enabled us to gain a better understanding of the periodic changes in vegetation in agricultural areas and their effects on canopy cover. In addition, the investigation attempted to assess the applicability of canopy cover estimations using high-resolution satellite images to distinguish between LCT types based on physical block ground truth (Table 4). There were significant changes in canopy cover rates between July 4, 2024, and August 24, 2024, for each land use type ( $P<0.05$ ).

**Table 3.** Descriptive statistics results for canopy cover effects on land cover in different periods

Variable	LCT	N	Minimum	Mean	Maximum	StDev	CoefVar	Skewness	Kurtosis
Canopy Cover (%)	A0	5425	3.187	33.531	73.659	11.967	35.69	0.46	-0.38
	A1	19	18.70	28.97	53.12	8.27	28.54	1.52	2.88
	A3	26	26.99	40.97	57.30	8.45	20.63	0.34	-0.62
	A4	13	7.91	28.39	43.05	11.93	42.02	-0.72	-0.79
	S1	20	25.43	39.37	53.41	8.12	20.62	0.02	-0.81
	T0	2878	8.632	45.226	74.677	10.634	23.51	-0.45	-0.17
Canopy Cover(%)	T1	7	39.19	53.87	65.78	11.49	21.32	-0.34	-1.80
	A0	5425	-3.163	21.157	78.132	16.974	80.23	1.03	0.01
	A1	19	3.18	18.08	40.81	10.33	57.13	0.90	-0.19
	A3	26	17.14	38.12	55.76	9.90	25.96	-0.24	-0.60
	A4	13	-0.65	26.97	51.37	15.48	57.42	-0.28	-0.79
	S1	20	13.36	35.28	66.14	13.45	38.14	0.37	-0.13
	T0	2878	2.020	45.768	76.189	15.163	33.13	-0.60	-0.41
	T1	7	26.82	45.26	64.57	14.51	32.07	0.11	-1.80

**Table 4.** ANOVA and Tukey test results for canopy cover effects on land cover in different periods

LCT	Physical Blocks	4 July 2024 CC (%) (Mean±SE)	24 August 2024 CC (%) (Mean±SE)
A0	5425	53.87±0.16 <sup>B</sup>	21.16±0.23 <sup>C</sup>
A1	19	45.23±1.90 <sup>B</sup>	18.08±2.37 <sup>C</sup>
A3	26	40.97±1.66 <sup>B</sup>	38.12±1.94 <sup>AB</sup>
A4	13	39.37±3.31 <sup>B</sup>	26.97±4.29 <sup>BC</sup>
S1	20	33.53±1.82 <sup>AB</sup>	35.28±3.01 <sup>AB</sup>
T0	2878	28.97±0.199 <sup>A</sup>	45.77±0.28 <sup>A</sup>
T1	7	28.39±4.34 <sup>A</sup>	45.26±5.49 <sup>AB</sup>

\* Capital letters indicate the difference between canopy cover averages for each land use ( $P<0.05$ ).

Table 4 shows a significant difference between the LCT groups in canopy cover estimates on July 4, 2024 and August 24, 2024 ( $P<0.05$ ). A substantial difference was found between "T0" and "A0 and A1" in both times ( $P<0.05$ ). A substantial difference was found between "T1" and "A0 and A1" in both times ( $P<0.05$ ). There was no statistically significant difference found between the plant species grown in groups A3, A4, and S1 and those grown in groups A0, A1, T0, and T1. This could also be due to parallel plant growth processes, which are expected to result in similar canopy cover levels. In addition, it is believed that this is related to the fact that the number of physical blocks in the research region for the A3, A4, and S1 land cover groups is less than that of the A0 and T0 groups.

#### 4. Discussion

The temperature and rainfall in the study area significantly varied between 2022 and 2023. Precipitation trends tend to fluctuate. Significant decreases were observed in January and February, whereas significant increases were observed in May, September, November, and December. These oscillations can be used to predict seasonal and climate changes. Temperatures vary similarly, with considerable increases in January and March and decreases in April and May. Temperatures rose modestly throughout the second half of the year. These changes reflect the climate's dynamic structure and are crucial data to consider for future climate analyses and environmental planning. Climate change also has a significant impact on agriculture. While changes in phenological periods cause shifting growing seasons and fluctuations in productivity in annual plants, precipitation and temperature changes during the flowering period in perennial plants have a negative impact on development and productivity due to issues with fruit set and quality. This situation is of critical importance in terms of agricultural production and sustainability (Talsma et al., 2018; Nhémachena et al., 2020; Revzi et al., 2023; Kazemi Garajeh et al., 2023; Qin et al., 2023; Carealla et al., 2024). Climatic changes in the research area in 2023 reduced apple production, which was grown in 91.7% of fruit farming areas by 20,521 tons. This increased 11503 tons in wheat and barley plant yields throughout 78.82% of grain fields (TurkStat, 2024). This circumstance stresses the importance of

changing agricultural production patterns in response to global climate change or switching to agricultural products appropriate for phenological times. In studies conducted with different apple varieties grown in Isparta province and its districts, it has been reported that full flowering dates are distributed in April and May (Uçgun and Gezgin, 2017; Eskimez et al., 2020; Küçükümuk, 2021; Küçükümuk and Erdal, 2022). In the study area's agricultural land use, apple cultivation is practiced in the majority of the fruit-growing areas, and the drop in yield is attributed to an increase in precipitation and a decrease in temperature in May 2023, the full flowering time. It has been stated that under Isparta climatic conditions, the wheat plant is in its development period in March, April, and May; therefore, increased rainfall increases productivity (Akgün et al., 2011). The increase in precipitation during the development phase of wheat and barley plants, which are grown in most grain fields in March, April, and May, improved yield while delaying harvest. Other research findings corroborate the idea that changes in the study area's climate have varying effects on agricultural goods (Akgün et al. 2011; Uçgun and Gezgin, 2017; Eskimez et al., 2020; Küçükümuk, 2021; Küçükümuk and Erdal, 2022). Keeping track of these changes is critical for establishing sustainable food supplies, agricultural policies, and subsidies. As a result of the study conducted to determine the land cover change due to climate change using the high-resolution Planet Scope satellite image of the land use classes corresponding to agricultural lands in the LPIS database, it was determined that the LPIS physical block data can be used as field data. The CC estimation performed using an image of the research region obtained on July 4 revealed that the grain areas were not harvested because of climate change that occurred during the plant growth season, which delayed harvest maturity. It was discovered that CC values had dropped in grain fields harvested in August (Table 3). It has been reported in studies that machine learning and deep learning algorithms made with physical blocks can be determined with high accuracy in determining the land cover type of Türkiye from LPIS data (Şimşek and Durduran, 2022; Şimşek, 2023). As a result, land cover classes (A0, A1, A3, A4, S1, T0, T1) representing agricultural areas in the study area were employed as ground truth. The utility of this data in monitoring phenological changes in land cover caused by climate change was determined based

on a variance analysis of the average canopy values of the physical block values. The analysis results can be used to discriminate between fruit agricultural areas and grain areas based on canopy cover values estimated throughout both periods (Table 4). It has been established that canopy cover estimation can be used to determine land use. The results were found to be consistent with those from other investigations (Trouth et al., 2008; Tsakmakis et al., 2021; Thieme et al., 2024). The limited number of physical blocks in the A3, A4, and S1 land cover types identified in this study is assumed to be the cause of their low discrimination compared with other classes.

In the future, it will be of great importance to develop the necessary strategies for agricultural areas to adapt to climate change. These strategies include developing plant species that are resistant to climate change, improving irrigation techniques, and optimizing soil management practices. In addition, agricultural policies and subsidies need to be rearranged within the framework of adaptation to climate change to ensure the sustainability of agricultural production.

This study has shown that the use of the LPIS database and high-resolution satellite images is an effective method for determining the effects of climate change on agricultural land cover. Monitoring canopy cover values can be used as an important tool to monitor the effects of climate change on phenological changes. Thus, changes occurring in agricultural areas can be detected more quickly and accurately, and adaptation strategies can be implemented in a timely and effective manner.

## 5. Conclusion

In this study, canopy cover estimation of agricultural lands in the study area was performed using high-resolution PlanetScope satellite images at different temporal resolutions. Changes in climatic conditions and vegetation have led to significant differences in the canopy cover data. Analyses of images taken in July and August showed that canopy cover values vary significantly in different LCT categories. While a more homogeneous distribution was observed in the A0 and T0 categories, more variability and skewness were noted in the A1 and A4 categories.

Data obtained in July and August provided critical information for understanding temporal changes in canopy cover estimates and the effects of agricultural activities in the study area. The study results revealed that the canopy cover values of plant species in the A3, A4, and S1 categories did not differ significantly from those in the A0, A1, T0, and T1 categories. This situation can be explained by the impact of similar plant cultivation techniques. In addition, it was determined that the number of physical blocks in the A0 and T0 categories was the two highest groups, and discrimination could be made according to canopy cover estimation in both periods due to differences in land use and plant patterns.

CC estimations based on high-resolution satellite images can be useful for monitoring phenological changes in agricultural fields and designing agricultural policies. Therefore, constant monitoring and adaptation studies are critical for mitigating the effects of climate change on agricultural production and ensuring food security. In this regard, applying contemporary technologies and data analysis methodologies can help improve agricultural sustainability. It is also recommended that local and national remote sensing resources be rapidly deployed and made available as standard data types for monitoring and evaluation studies.

## Author Contributions

The percentage of the author contributions is presented below. The author reviewed and approved the final version of the manuscript.

	S.D.
C	100
D	100
S	100
DCP	100
DAI	100
L	100
W	100
CR	100
SR	100
PM	100
FA	100

C=Concept, D= design, S= supervision, DCP= data collection and/or processing, DAI= data analysis and/or interpretation, L= literature search, W= writing, CR= critical review, SR= submission and revision, PM= project management, FA= funding acquisition.

## Conflict of Interest

The author declared that there is no conflict of interest.

## Ethical Consideration

Ethics committee approval was not required for this study because of there was no study on animals or humans.

## Acknowledgments

We thank the General Directorate of Agricultural Reform of the Ministry of Agriculture and Forestry for supplying us with the Land Identification Parcel System (LPIS) PBLOCKS\_VPG\_D4c\_TM30\_areas data used in this study. Their support and collaboration were instrumental in the successful completion of this research. We also extend our appreciation to all individuals and institutions involved in the collection, processing, and dissemination of the data.

## References

- Akgün İ, Altindal D, Kara B. 2011. Determination of suitable sowing dates for some bread and durum wheat cultivars under Isparta ecological conditions. JAS, 17(4): 300-309.

- Aljanabi F, Dedeoğlu M, Şeker C. 2024. Environmental monitoring of Land Use/Land Cover by integrating remote sensing and machine learning algorithms. *J Eng Sustain Devel*, 28(4): 455-466.
- Anonymous. 2024. Republic of Türkiye Ministry of Agriculture and Forestry Agricultural Production Planning Group Work Document. URL: <https://cdniys.tarimorman.gov.tr/api/File/GetGaleriFile/330/DosyaGaleri/956/16%20Tar%C4%B1msal%20%C3%9Cretim%20%20Planlamas%C4%B1%20Grubu%20%C3%87al%C4%B1%C5%9Fma%20Belgesi.pdf> (accessed date: May 19, 2024).
- ArcGIS. 2024. ArcGIS Pro geoprocessing tool reference. URL: <https://pro.arcgis.com/en/pro-app/latest/tool-reference/main/arcgis-pro-tool-reference.htm> (accessed date: May 19, 2024).
- Baret F, Guyot G. 1991. Potentials and limits of vegetation indices for LAI and APAR assessment. *Remote Sens Environ*, 35(2-3): 161-173.
- Basso B, Cammarano D, De Vita P. 2004. Remotely sensed vegetation indices: Theory and applications for crop management. *Rivista Italiana di Agrometeorologia*, 1(5): 36-53.
- Berger K, Machwitz M, Kycko M, Kefauver SC, Van Wittenbergh S, Gerhards M, Verrelst J, Atzberger C, van der Tol C, Damm A, Rascher U, Herrmann I, Sobejano Paz V, Fahrner S, Pieruschka R, Prikaziuk E, Buchaillet ML, Halabuk A, Celesti M, Koren G, Tunc Gormus E, Rossini M, Foerster M, Siegmann B, Abdelbaki A, Tagliabue G, Hank T, Darvishzadeh R, Aasen H, Garcia M, Poças I, Bandopadhyay S, Sulis M, Tomelleri E, Rozenstein O, Filchev L, Stancile G, Schlerf M. 2022. Multi-sensor spectral synergies for crop stress detection and monitoring in the optical domain: A review. *Remote Sens Environ*, 280: 113198.
- Çakır M, Yıldırım A, Çelik C, Esen M. 2021. The effect of different plant growth regulators on the quality and biochemical content of Jerome apple cultivar. *Anadolu J Agri Sci*, 36(3): 478-487.
- Carella A, Bulacio Fischer PT, Massenti R, Lo Bianco R. 2024. Continuous plant-based and remote sensing for determination of fruit tree water status. *Horticulturae*, 10(5): 516.
- Clevers JGPW. 1989. Application of a weighted infrared-red vegetation index for estimating leaf area index by correcting for soil moisture. *Remote Sens Environ*, 29(1): 25-37.
- Damm A, Paul-Limoges E, Haghghi E, Simmer C, Morsdorf F, Schneider FD, van der Tol C, Migliavacca M, Rascher U. 2018. Remote sensing of plant-water relations: An overview and future perspectives. *J Plant Physiol*, 227: 3-19.
- Demir S, Başayıgit L. 2024. Digital mapping burn severity in agricultural and forestry land over a half-decade using sentinel satellite images on the Google earth engine platform: A case study in Isparta province. *Trees for People*, 16: 100520.
- Demir S, Dedeoğlu M, Başayıgit L. 2024. Yield prediction models of organic oil rose farming with agricultural unmanned aerial vehicles (UAVs) images and machine learning algorithms. *Remote Sens Appl*, 33: 1-25.
- Demir S. 2023. Determination of burned areas at different threshold values using Sentinel-2 satellite images on Google Earth Engine. *Turk J Remote Sens GIS*, 4(2): 262-275.
- Demir S. 2024. Determination of suitable agricultural areas and current land use in Isparta Province, Türkiye, through a linear combination technique and geographic information systems. *Environ Dev Sustain*, 26: 13455-13493.
- Erdas. 2024. How to create an NDVI image using Erdas Imagine. URL: [https://supportsi.hexagon.com/help/s/article/How-to/Create-an-NDVI-Image-using-ERDAS-IMAGINE?language=en\\_US](https://supportsi.hexagon.com/help/s/article/How-to>Create-an-NDVI-Image-using-ERDAS-IMAGINE?language=en_US) (accessed date: May 19, 2024).
- Esetlili M T, Serbeş Z A, Çolak Esetlili B, Kurucu Y, Delibacak S. 2022. Determination of water footprint for the cotton and maize production in the Küçük Menderes Basin. *Water*, 14(21): 3427.
- Eskimez İ, Polat M, Mertoğlu K. 2020. Phenological and physico-chemical characteristics of Arapkırı, Jonagold and Fuji Kiku Apple (*Malus domestica* Bork.) varieties grafted on M9 rootstock in Isparta ecological conditions. *Uluslararası Tarım Yaban Hayatı Bil Derg*, 6(2): 152-159.
- Ghiat I, Mackey HR, Al-Ansari T. 2021. A review of evapotranspiration measurement models, techniques and methods for open and closed agricultural field applications. *Water*, 13(18): 2523.
- Ghuffar S. 2018. DEM generation from multi-satellite PlanetScope imagery. *Remote Sens*, 10(9): 1462.
- Gitelson AA. 2013. Remote estimation of crop fractional vegetation cover: the use of noise equivalent as an indicator of performance of vegetation indices. *Int J Remote Sens*, 34(17): 6054-6066.
- Gong H, Cheng Q, Jin H, Ren Y. 2023. Effects of temporal, spatial, and elevational variation in bioclimatic indices on the NDVI of different vegetation types in Southwest China. *Ecol Indic*, 154: 110499.
- Hassan MA, Yang M, Rasheed A, Jin X, Xia X, Xiao Y, He Z. 2018. Time-series multispectral indices from unmanned aerial vehicle imagery reveal senescence rate in bread wheat. *Remote Sens*, 10(6): 809.
- Hatfield JL, Prueger JH, Sauer TJ, Dold C, O'Brien P, Wacha K. 2019. Applications of vegetative indices from remote sensing to agriculture: Past and future. *Inventions*, 4(4): 71.
- Huete AR. 1988. A soil-adjusted vegetation index (SAVI). *Remote Sens Environ*, 25(3): 295-309.
- Kaufman YJ, Tanre D. 1992. Atmospherically resistant vegetation index (ARVI) for EOS-MODIS. *IEEE Trans Geosci Remote Sens*, 30(2): 261-270.
- Kazemi Garajeh M, Salmani B, Zare Naghadehi S, Valipoori Goodarzi H, Khasraei A. 2023. An integrated approach of remote sensing and geospatial analysis for modeling and predicting the impacts of climate change on food security. *Sci Rep*, 13(1): 1057.
- Küçükuyumuk Z, Erdal İ. 2022. Effect of calcium on and mineral nutrient concentrations and fruit quality in different apple tree varieties. *J Elem*, 27(1): 75-85.
- Küçükuyumuk Z. 2021. Foliarly applied osmotic preservative contributes to pear (*Pyrus communis*) leaf and root nutritional status under drought stress. *Appl Ecol Environ Res*, 19(4): 3019-3028.
- Kumar V, Sharma A, Bhardwaj R, Thukral AK. 2018. Comparison of different reflectance indices for vegetation analysis using Landsat-TM data. *Remote Sens Appl*, 12: 70-77.
- Kumar V, Sharma KV, Pham QB, Srivastava AK, Bogireddy C, Yadav SM. 2024. Advancements in drought using remote sensing: assessing progress, overcoming challenges, and exploring future opportunities. *Theor Appl Climatol*, 2024: 1-38.
- Le TS, Harper R, Dell B. 2023. Application of remote sensing in detecting and monitoring water stress in forests. *Remote Sens*, 15(13): 3360.
- Ličina V, Krogstad T, Fotirić Akšić M, Meland M. 2024. Apple growing in Norway-ecologic factors, current fertilization

- practices and fruit quality: a case study. *Horticulturae*, 10(3): 233.
- MGM. 2024. General Directorate of Meteorology, Turkish State Meteorological Service. URL: <https://www.mgm.gov.tr/veridegerlendirme/il-ve-ilceler-istatistik.aspx?m=ISPARTA> (accessed date: May 19, 2024).
- Minitab. 2024. Minitab statistical software. URL: <https://www.minitab.com/en-us/products/minitab/free-trial/> (accessed date: May 19, 2024).
- Nhemachena C, Nhamo L, Matchaya G, Nhémachena CR, Muchara B, Karuaihe ST, Mpandeli S. 2020. Climate change impacts on water and agriculture sectors in Southern Africa: Threats and opportunities for sustainable development. *Water*, 12(10): 2673.
- Oliveira S, Cunha J, Nóbrega RL, Gash JH, Valente F. 2024. Enhancing global rainfall interception loss estimation through vegetation structure modeling. *J Hydrol*, 631: 130672.
- Pei F, Wu C, Liu X, Li X, Yang K, Zhou Y, Wang K, Xu L, Xia G. 2018. Monitoring the vegetation activity in China using vegetation health indices. *Agric For Meteorol*, 248: 215-227.
- Pinty B, Verstraete MM. 1992. GEMI: a non-linear index to monitor global vegetation from satellites. *Vegetatio*, 101:15-20.
- Planet. 2024. Planet imagery product specifications. URL: [https://assets.planet.com/docs/Planet\\_Combined\\_Imagery\\_Product\\_Specs\\_letter\\_screen.pdf](https://assets.planet.com/docs/Planet_Combined_Imagery_Product_Specs_letter_screen.pdf) (accessed date: May 19, 2024).
- Qin S, Li S, Cheng L, Zhang L, Qiu R, Liu P, Xi H. 2023. Partitioning evapotranspiration in partially mulched interplanted croplands by improving the Shuttleworth-Wallace model. *Agric For Meteorol*, 276: 108040.
- Rezvi HUA, Tahjib-Ul-Arif M, Azim MA, Tumpa TA, Hasan Tipu MM, Najnine F, Dawood MFA, Skalicky M, Brestić M. 2023. Rice and food security: Climate change implications and the future prospects for nutritional security. *Food Energy Secur*, 12(1): e430.
- Rondeaux G, Steven M, Baret F. 1996. Optimization of soil-adjusted vegetation indices. *Remote Sens Environ*, 55(2): 95-107.
- Rouse JW, Haas RH, Schell JA, Deering DW. 1974. Monitoring vegetation systems in the Great Plains with ERTS. NASA Spec. Publ., New York, US, 351(1): 309-330.
- Selim S, Sönmez NK, Çoşlu M. 2022. The effect of temporal variation in land surface temperature on land cover classes and agricultural areas: Recent Studies in Planning and Design. İKSAD Publishing House, Ankara, Türkiye, 1th ed., pp: 183-207.
- Selim S, Sönmez NK. 2015. Determination of sweetgum (*Liquidambar orientalis* Miller) populations distribution with geographic information systems and evaluation of landscape metrics by using habitat quality assessment; a case study of Mugla Koycegiz. *Tekirdağ Zir Fak Derg*, 12(1): 30-38.
- Seong S, Chang A, Mo J, Na S, Ahn H, Oh J, Choi J. 2024. Crop classification in South Korea for multitemporal PlanetScope imagery using SFC-DenseNet-AM. *Int J Appl Earth Obs Geoinf*, 126: 103619.
- Şimşek FF 2023. Land cover and land use classification at national scale using Land Parcel Identification System Data (LPIS). *Turk J Remote Sens GIS*, 4(2): 276-288.
- Şimşek FF, Durduran SS. 2022. Land cover classification using Land Parcel Identification System (LPIS) data and open source Eo-Learn library. *Geocarto Int*, 38: 1-18.
- Talsma CJ, Good SP, Jimenez C, Martens B, Fisher JB, Miralles DG, McCabe MF, Purdy AJ. 2018. Partitioning of evapotranspiration in remote sensing-based models. *Agric For Meteorol*, 260: 131-143.
- Team P. 2017. Planet application program interface: In space for life on Earth. San Francisco, US, pp: 67.
- Tenreiro TR, García-Vila M, Gómez JA, Jiménez-Berni JA, Fereres E. 2021. Using NDVI for the assessment of canopy cover in agricultural crops within modelling research. *Comput Electron Agri*, 182: 106038.
- Thieme A, Prabhakara K, Jennewein J, Lamb BT, McCarty GW, Hively WD. 2024. Intercomparison of same-day remote sensing data for measuring winter cover crop biophysical traits. *Sensors*, 24(7): 1-25.
- Trout TJ, Johnson LF, Gartung J. 2008. Remote sensing of canopy cover in horticultural crops. *Hort Sci*, 43(2): 333-337.
- Trout TJ, Johnson LF. 2007. Estimating crop water use from remotely sensed NDVI. crop models. and reference ET. USCID Fourth International Conference on Irrigation and Drainage, October 3-6, Sacramento, California, US, pp: 275-285.
- Tsakmakis ID, Gikas GD, Sylaios GK. 2021. Integration of Sentinel-derived NDVI to reduce uncertainties in the operational field monitoring of maize. *Agri Water Manag*, 255: 106998.
- Tucker CJ. 1979. Red and photographic infrared linear combinations for monitoring vegetation. *Remote Sens Environ*, 8(2): 127-150.
- Uçgun K, Gezgin S. 2017. Interpretation of leaf analysis performed in early vegetation in apple orchards. *Commun Soil Sci Plant Anal*, 48(14): 1719-1725.
- Vos K, Harley MD, Splinter KD, Simmons JA, Turner IL. 2019. Sub-annual to multi-decadal shoreline variability from publicly available satellite imagery. *Coast Eng*, 150: 160-174.
- Yalçın B, Yıldırım A, Yıldırım F, Çelik C. 2021. Biochemical and mineral contents of some walnut cultivars in Isparta ecology. *ADÜ Zir Derg*, 18(2): 285-291.
- Yılmaz R, Yıldırım A, Çelik C, Karakurt Y. 2021. Determination of nut characteristics and biochemical components of some pecan nut cultivars. *YYU J Agri Sci*, 31(4): 906-914.